Eur. Phys. J. B **17**, 515–521 (2000)

THE EUROPEAN PHYSICAL JOURNAL B

EDP Sciences

Compressibility crossover and quantum opening of a gap for two-dimensional disordered clusters with Coulomb repulsion

G. Benenti[1], X. Waintal[1], J.-L. Pichard[1,a], and D.L. Shepelyansky[2]

[1] CEA, Service de Physique de l'État Condensé, Centre d'Études de Saclay, 91191 Gif-sur-Yvette, France
[2] Laboratoire de Physique Quantique[b], Université Paul Sabatier, 31062 Toulouse, France

Received 13 March 2000

Abstract. Using Hartree-Fock orbitals with residual Coulomb repulsion, we study spinless fermions in a two-dimensional random potential. When we increase the system size L at fixed particle density, the size dependence of the average inverse compressibility exhibits a smooth crossover from a $1/L^2$ towards a $1/L$ decay when the Coulomb energy to Fermi energy ratio r_s increases from 0 to 3. In contrast, the distribution of the first energy excitation displays a sharp Poisson-Wigner-like transition at $r_s \approx 1$.

PACS. 71.30.+h Metal-insulator transitions and other electronic transitions – 72.15.Rn Localization effects (Anderson or weak localization)

1 Introduction

The interplay of disorder and interactions in two dimensional (2d) electronic systems is currently a central problem in condensed matter physics [1]. The importance of interactions is illustrated by several phenomena, notably Coulomb repulsion could be crucial in understanding the observation of a metallic phase in various two-dimensional devices [2], since the metal-insulator transition occurs at a large Coulomb energy to Fermi energy ratio $r_s \approx 10$. Compressibility measurements indicate that the high r_s insulating phase is incompressible [3] and spatially inhomogeneous [4].

In weakly disordered quantum dots, the inverse compressibility gives the spacing between adjacent conductance peaks. The peak spacing statistics, obtained in experiments in which $r_s \approx 1$, displays fluctuations larger than those predicted from Random Matrix Theory, characterized by a Gaussian-like distribution instead of a Wigner-Dyson distribution [5–7]. This suggests a breakdown of the naive single particle picture, assumed in the constant interaction model.

In strongly disordered insulators, the long range nature of interactions leads to a soft Coulomb gap in the single particle density of states at the Fermi level [8], observed in tunneling spectroscopic experiments in 3d [9] and 2d [10] nonmetallic semiconductors. Assuming that single electron hoppings dominate the transport, the Coulomb gap leads to a crossover in the temperature dependence of the resistivity $\rho(T)$ from the Mott variable range hopping law ($\rho(T) = \rho_M \exp(T_0/T)^{1/3}$ in dimension $d = 2$) to the Efros-Shklovskii behavior ($\rho(T) = \rho_{ES} \exp(T_{ES}/T)^{1/2}$) [8]. This crossover has been reported [11] not only by decreasing the temperature but also by decreasing the carrier density (around $r_s \approx 1.7$).

In this paper, we numerically investigate the physics of 2d Coulomb interacting spinless fermions in a random potential for relatively low values of the factor r_s (≤ 3), when the single particle spectra display either Wigner-Dyson statistics for weak disorder (diffusion) or Poisson statistics for strong disorder (Anderson localization). As exact diagonalization studies are restricted to small system sizes [12], we use a numerical method [13,14] familiar in quantum chemistry as the configuration interaction method (CIM) [15]. The method consists in diagonalizing the Hamiltonian in an energetically truncated basis built of the low-energy states of the corresponding Hartree-Fock (HF) Hamiltonian. This method allows us to study the ground state and the lowest energy excitations for different system sizes L at constant electronic density.

We show that the average inverse compressibility Δ_2 exhibits a smooth crossover from a $1/L^2$ towards a $1/L$ decay when r_s increases from 0 to 3. The first dependence corresponds to the average single particle level spacing without interaction while the latter refers to the charging energy. At the same time, the distribution of Δ_2 evolves from the Wigner-Dyson distribution (or the Poisson distribution, if disorder is strong enough or L large enough) towards a Gaussian-like shape. Therefore fluctuations in Δ_2 are determined by Coulomb repulsion rather than from single particle level fluctuations.

We have also studied the energy level spacing between the ground state and the first excitation for strongly disordered clusters: the average indicates a smooth opening

[a] e-mail: pichard@spec.saclay.cea.fr
[b] UMR C5626 du CNRS

of a gap when r_s increases, while the distribution exhibits a sharp Poisson-Wigner-like transition at $r_s = r_s^C \approx 1.2$. The critical threshold r_s^C is characterized by a scale invariant gap distribution, reminiscent of the one particle problem [16] at a mobility edge. However, it is only the distribution of the first spacing which exhibits such a transition, the distributions of the next spacings remain Poissonian and are essentially unchanged when r_s varies.

The paper is organized as follows: in Section 2 we introduce the model, in Section 3 we discuss the numerical technique used and its limits of validity; in Section 4 we present our compressibility data; in Section 5 we discuss the statistical properties of the lowest energy excitations; in Section 6 we discuss the implications of our results for hopping conductivity experiments; in Section 7 we present our conclusions.

2 The model

We consider a disordered square lattice with $M = L^2$ sites occupied by N spinless fermions. The Hamiltonian reads

$$H = -t \sum_{\langle i,j \rangle} c_i^\dagger c_j + \sum_i v_i n_i + U \sum_{i \neq j} \frac{n_i n_j}{2 r_{ij}}, \qquad (1)$$

where $c_i^\dagger$ (c_i) creates (destroys) an electron in the site i, the hopping term t between nearest neighbors characterizes the kinetic energy, v_i the site potentials taken at random inside the interval $[-W/2, +W/2]$, $n_i = c_i^\dagger c_i$ is the occupation number at site i and U measures the strength of the Coulomb repulsion. The boundary conditions are periodic and r_{ij} is the inter-particle distance for a 2d torus. If $a_B^* = \hbar^2 \epsilon / (m^* e^2)$, m^*, ϵ, a and $n_s = N/(aL^2)$ denote respectively the effective Bohr radius, the effective mass, the dielectric constant, the lattice spacing and the carrier density, the factor r_s is given by:

$$r_s = \frac{1}{\sqrt{\pi n_s} a_B^*} = \frac{U}{2t\sqrt{\pi n_e}}, \qquad (2)$$

since in our units $\hbar^2/(2m^*a^2) \to t$, $e^2/(\epsilon a) \to U$ and $n_e = N/L^2$.

3 Configuration interaction method

A numerical study of the model (1) *via* exact diagonalization techniques for sparse matrices is possible only for small systems [12], and does not allow us to vary L for a constant density. We are obliged to look for an approximate solution of the problem, using the Hartree-Fock orbitals, and to control the validity of the approximations. One starts from the HF Hamiltonian where the two-body part is reduced to an effective single particle Hamiltonian [17–19]

$$U \left(\sum_{i \neq j} \frac{1}{r_{ij}} n_i \langle n_j \rangle - \sum_{i \neq j} \frac{1}{r_{ij}} c_i^\dagger c_j \langle c_j^\dagger c_i \rangle \right), \qquad (3)$$

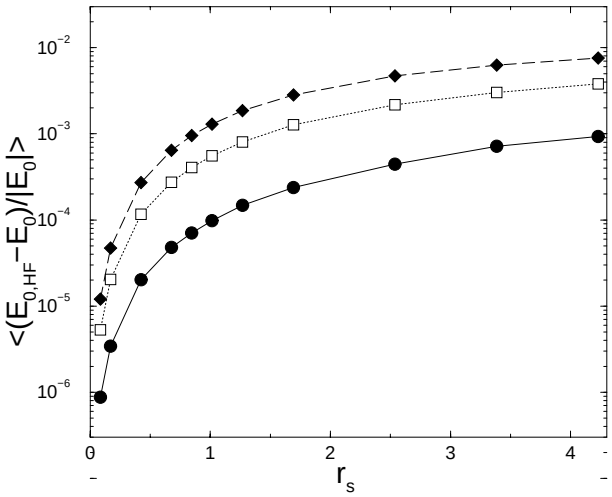

Fig. 1. Relative error in the HF ground state energy as a function of r_s, for $N = 4$, $L = 6$, $W = 15$ (circles), $W = 8$ (squares), and $W = 5$ (diamonds). The contribution of a positive uniform background has been included in the energies. Brackets indicate disorder average (here over 10^2 configurations).

where $\langle ... \rangle$ stands for the expectation value with respect to the HF ground state, which has to be determined self-consistently. For large values of the interaction and large system sizes the single-particle problem (3) is still non-trivial, since the self-consistent iteration can be trapped in metastable states. This limits our study to small r_s and forbids us to study by this method charge crystallization discussed in [12] at a larger $r_s^W \approx 10$.

Figure 1 shows that the HF ground state energy $E_{0,HF}$ gives a good estimate of the exact ground state energy E_0. This approximation becomes worse for (1) larger interactions or (2) smaller disorder. The first characteristic is due to the fact that the ground state HF energy is exact in the limits $U \to 0$ and $U \to \infty$, in which the ground state is given by a single Slater determinant, but deviations from this simple picture are expected at intermediate U values. The latter feature can be understood as complicated many-body screening effects, which are effective up to a distance of the order of the localization length, cannot be reproduced within simple HF.

The main advantage of the HF approximation is that it reproduces well the single particle density of states [19], particularly the soft Coulomb gap at the Fermi energy [8]. However, the approximations involved in the HF method are uncontrolled. The mean field HF results can be improved using the configuration interaction method [13–15]. Once a complete orthonormal basis of HF orbitals has been calculated:

$$H_{HF}(|\psi_1\rangle, ..., |\psi_N\rangle)|\psi_\alpha\rangle = \epsilon_\alpha |\psi_\alpha\rangle, \qquad (4)$$

with $\alpha = 1, 2, \ldots, L^2$, it is possible to build up a Slater determinants' basis for the many-body problem which can be truncated to the N_H first Slater determinants, ordered by increasing energies. The two-body Hamiltonian can be

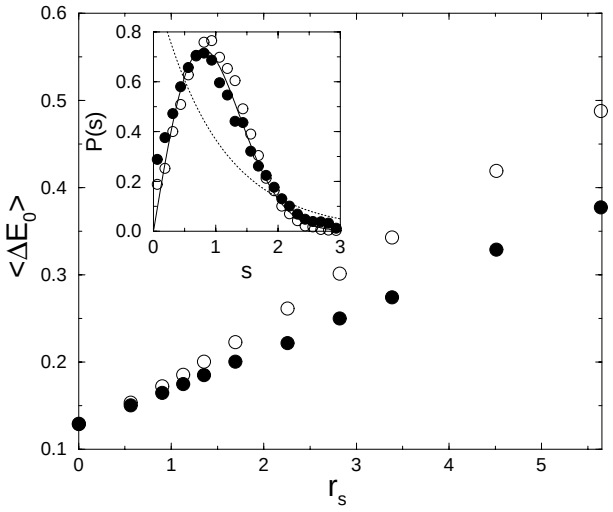

Fig. 2. CIM result (filled circles) compared to HF approximation (empty circles) for $N = 9$, $L = 12$, $W = 15$. Mean gap $\langle \Delta E_0 \rangle$ and gap distribution at $r_s = 4.5$ (inset). Disorder average is over 10^4 configurations.

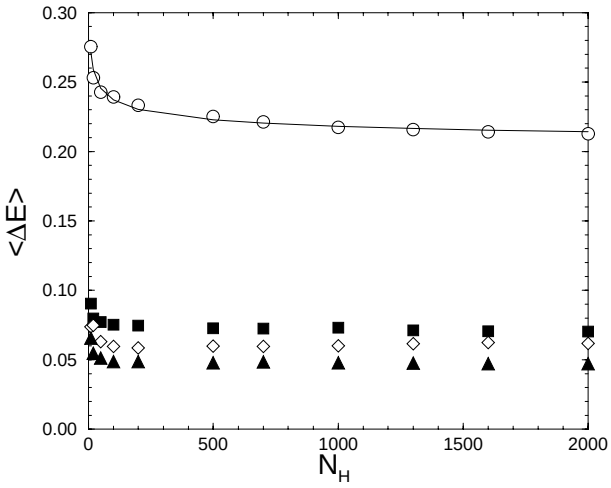

Fig. 3. First (circles), second (squares), third (diamonds), and fourth (triangles) average spacing as a function of the size N_H of the truncated Hilbert space, for $N = 16$, $L = 16$, $W = 15$, $r_s = 2.8$. The first gap is fitted by the curve $\langle \Delta E_0 \rangle = 0.195 + 0.13 N_H^{-0.26}$; therefore one can estimate the relative error at $N_H = 2 \times 10^3$ as $< 10\%$. Disorder average is over 10^2 configurations.

written as

$$H_{\rm int} = \frac{1}{2} \sum_{\alpha,\beta,\gamma,\delta} Q^{\gamma\delta}_{\alpha\beta} d^\dagger_\alpha d^\dagger_\beta d_\delta d_\gamma, \tag{5}$$

with

$$Q^{\gamma\delta}_{\alpha\beta} = U \sum_{i \neq j} \frac{\psi_\alpha(i)\psi_\beta(j)\psi_\gamma(i)\psi_\delta(j)}{r_{ij}} \tag{6}$$

and $d^\dagger_\alpha = \sum_j \psi_\alpha(j) c^\dagger_j |0\rangle$. One gets the residual interaction subtracting equation (3) from equation (5). This keeps the two-body nature of the Coulomb interaction, and if $N \gg 2$ it is still possible to take advantage of the sparsity of the matrix and to diagonalize it *via* the Lanczos algorithm.

Figure 2 compares HF and CIM results. Labelling the N-body levels E_i $(i = 0, 1, 2, ...)$ by increasing energy we have studied the first spacing $\Delta E_0 = E_1 - E_0$. When $r_s > 1$, the residual interaction significantly reduces the mean gap, and slightly changes its distribution. Within HF approximation, the first excitation is a particle-hole excitation starting from the ground state: The mean gap reduction is due to correlation effects beyond the particle-hole interaction. For example, the electron (hole) polarizes its neighborhood as it creates fluctuations in the local charge density.

We have checked that CIM results agree with the results given from exact diagonalization with an accuracy of the order 2% when one takes into account the $N_H = 10^3$ lowest energy Slater determinants when $N = 4$, $L = 8$, $W = 15$, and $r_s = 5$. This means that a basis spanning only 0.2% of the total Hilbert space is sufficient for studying the first excitations. For larger L, exact diagonalization is no longer possible, but one can look the variation of the results when N_H increases. In the worst case considered ($N = 16$, $L = 16$, $W = 15$, $r_s = 2.8$) the accuracy in the first four spacings can be estimated as better than 10% when $N_H = 2 \times 10^3$ (see Fig. 3).

Therefore the CIM method allows to study low energy level statistics for $r_s < 3$. However, its accuracy is not sufficient to determine more sensitive quantities, like a small change of the ground state energy when the boundary conditions are twisted (*i.e.* the persistent currents).

4 Electronic compressibility

In quantum dots experiments in the Coulomb blockade regime the spacing between consecutive conductance peaks is given by

$$\Delta_2(N) = E_0(N+1) - 2E_0(N) + E_0(N-1), \tag{7}$$

with $E_0(N)$ N-body ground state. This quantity is the discretized second derivative of the ground state energy with respect to the number of particles, *i.e.* the inverse compressibility. In the constant interaction model, which ignores fluctuations in the Coulomb energy

$$Q^{\gamma\delta}_{\alpha\beta} = \frac{e^2}{C} \delta_{\alpha\gamma} \delta_{\beta\delta}, \tag{8}$$

where C is the capacitance of the dot. This gives $E_0(N) = e^2 N(N-1)/2C + \sum_{k=1}^{N} \eta_k$, where η_k is the kth single particle energy at $U = 0$. Substituting this expression into equation (7) one finds $\Delta_2 = e^2/C + \eta_{N+1} - \eta_N$. Random Matrix Theory describes the single particle level spacings when the disorder is weak. The peak spacing distribution is expected to follow the Wigner-Dyson distribution with fluctuations in Δ_2 whose standard deviation is given by $\delta\Delta_2 \equiv \sqrt{\langle \Delta_2^2 \rangle - \langle \Delta_2 \rangle^2} = \sqrt{4/\pi - 1} \langle \Delta \rangle \approx 0.52 \langle \Delta \rangle$, where $\langle \Delta \rangle$ is the single particle mean level spacing. However,

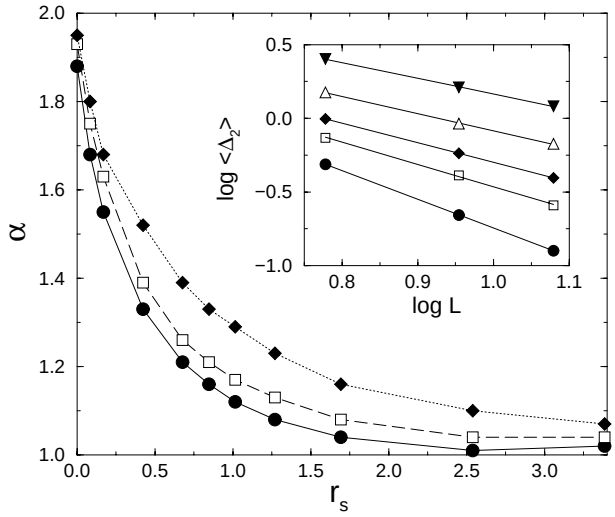

Fig. 4. Inset: size dependence of the average inverse compressibility $\langle \Delta_2 \rangle$, for $W = 15$, filling factor $n_e = 1/9$, $r_s = 0$ (circles), 0.4 (squares), 0.8 (diamonds), 1.7 (triangles up), and 3.4 (triangles down). Straight lines are power law fits $\langle \Delta_2(r_s) \rangle \propto L^{-\alpha(r_s)}$. Main figure: Exponent $\alpha(r_s)$ for $n_e = 1/9$, $W = 5$ (circles), $W = 8$ (squares), and $W = 15$ (diamonds). Disorder average for the compressibility data is over 10^3 configurations.

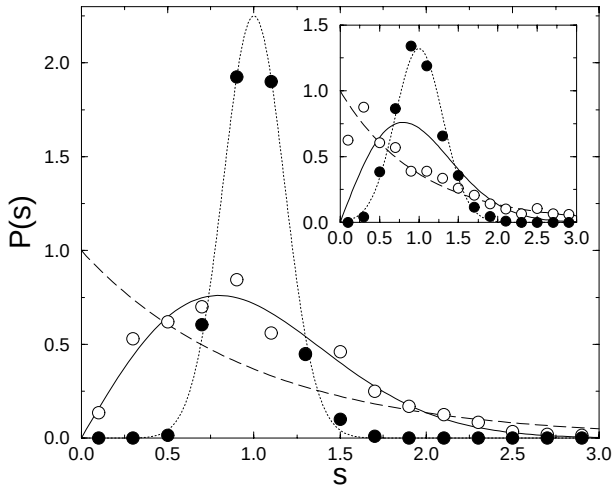

Fig. 5. Distribution of the normalized inverse compressibilities for $N = 16$, $L = 12$, $W = 5$, $r_s = 0$ (empty circles) and $r_s = 2.5$ (filled circles), fitted by a Gaussian of standard deviation $\sigma = 0.18$ (dotted line). Solid and dashed lines give Wigner and Poisson distribution respectively. Inset: same at $W = 15$; the Gaussian fit gives $\sigma = 0.30$.

experiments [5–7] performed at $r_s \approx 1$ found a distribution which is Gaussian-like and has a larger width, up to 7.5Δ [7]. This suggests that fluctuations in Δ_2 are dominated by electron-electron interactions. Several observed features of the peak spacing distributions have been reproduced using exact numerical diagonalization of the Hamiltonian model (1) [5], HF calculations [20–22], and a random matrix model for interacting fermionic systems [23].

In this paper we study the inverse compressibility at different system sizes, for a constant filling factor $n_e = 1/9$. We consider $N = 4, 9, 16$ particles on square lattices of size $L = 6, 9, 12$ respectively. A Fermi golden rule approximation for the elastic scattering time gives [21], for $n_e \ll 1$, $k_F l \approx 192\pi n_e (t/W)^2$, k_F and l denoting the Fermi wave vector and the elastic mean free path, respectively. We consider $W = 5, 8, 15$, corresponding to $k_F l \approx 2.7, 1, 0.3$; the first case corresponds to a diffusive system ($L > l/a \approx 2.3$, with a lattice spacing), the last one to a strongly localized system.

The following inverse compressibility data are obtained with the CIM. We have checked that the residual interaction does not change qualitatively HF results. This is consistent with Figure 1: HF approximation gives a good estimate of the ground state energy and the inverse compressibility is a physical observable which depends only on the ground state energies at different number of particles. Neither a precise knowledge of the ground state wavefunction (as in the calculation of persistent currents) nor excited states energies (as in studies of spectral statistics) are required.

Figure 4 shows the L-dependence of the average inverse compressibility, which is well fitted by the power law $< \Delta_2(r_s) > \propto L^{-\alpha(r_s)}$, with $\alpha(r_s)$ going from 2 to 1 when r_s goes from 0 to 3 approximately. The value $\alpha = 2$ is expected without interaction ($\langle \Delta_2 \rangle = \langle \Delta \rangle \propto 1/L^2$). The exponent $\alpha = 1$ can be understood as follows: for $r_s > 1$, Δ_2 is dominated by the charging energy and therefore $\langle \Delta_2 \rangle \propto 1/C \propto 1/L$. In the strongly localized regime ($W = 15$) the $1/L$ law is justified due to the Coulomb gap in the single particle density of states [8]: According to Koopmans' theorem [24], assuming that the other charges are not reorganized by the addition of an extra charge,

$$\Delta_2 \approx \epsilon_{N+1} - \epsilon_N \propto \frac{1}{L} \tag{9}$$

due to the Coulomb gap, where ϵ_k is the energy of the kth HF orbital at a fixed number N of particles.

Figure 5 shows the distribution of inverse compressibilities, for $L = 12$, $W = 5$ and $W = 15$ (inset). At $r_s = 0$, Δ_2 distributions are close to the Wigner surmise $P_W(s = \Delta_2/\langle \Delta_2 \rangle) = (\pi s/2) \exp(-\pi s^2/4)$ for $W = 5$ and to the Poisson distribution $P_P(s) = \exp(-s)$ for $W = 15$. In the latter case, deviations from the Poisson distribution at small s values are due to the finite system size. In both cases at $r_s = 2.5$ distributions show a Gaussian shape. This can be understood within the Koopmans' theorem, as the HF energies are given by

$$\epsilon_k = \langle \psi_k | H_1 | \psi_k \rangle + \sum_{\alpha=1}^{N} \left(Q_{\alpha k}^{\alpha k} - Q_{\alpha k}^{k \alpha} \right), \tag{10}$$

with H_1 one-body part of the Hamiltonian (1): Due to the small correlations of eigenfunctions in a random potential, one can reasonably invoke the central limit theorem (see Ref. [22] for a more detailed discussion).

Figure 6 shows the r_s-dependence of the inverse compressibility standard deviation $\delta\Delta_2$, normalized to the single particle mean level spacing $\langle \Delta \rangle$. One can see that

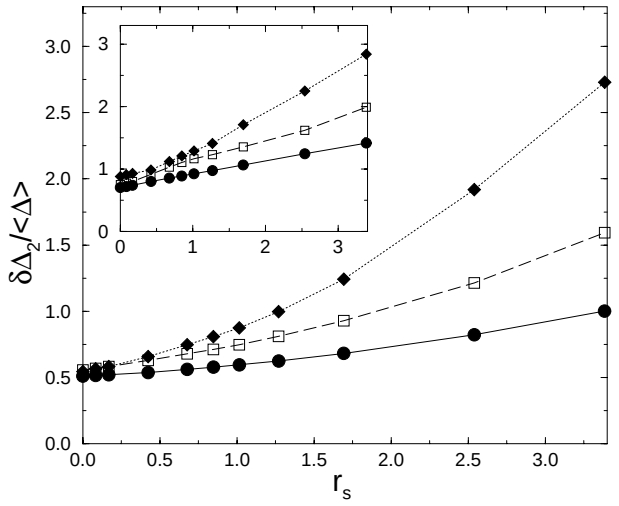

Fig. 6. Inverse compressibility standard deviation $\delta\Delta_2$, normalized to the single particle mean level spacing $\langle\Delta\rangle$ as a function of r_s, for $W = 5$, $n_e = 1/9$, $L = 6$ (circles), $L = 9$ (squares), and $L = 12$ (diamonds). Inset: same at $W = 15$.

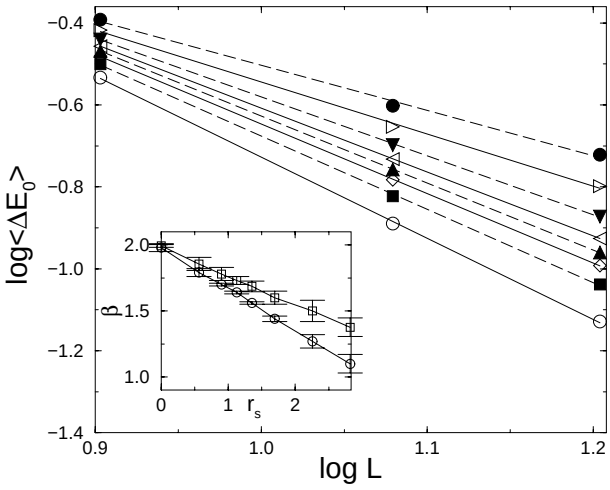

Fig. 7. Size dependence of the average gap (first spacing $\langle\Delta E_0\rangle \propto L^{-\beta(r_s)}$), for $W = 15$, filling factor $n_e = 1/16$. From bottom to top: $r_s = 0, 0.6, 0.9, 1.1, 1.4, 1.7, 2.3, 2.8$. Inset: $\beta(r_s)$ (circles, characterizing $\langle\Delta E_0\rangle$ and squares, characterizing $\langle\Delta E_i\rangle$, with an average over $i = 1 - 3$). Disorder average is over 10^4 configurations.

$\delta\Delta_2/\langle\Delta\rangle$ increases slowly for $r_s < 1$ and then more rapidly with r_s growth. This results are in contrast with random phase approximation estimates [25,26], giving fluctuations of the order Δ. On the contrary, we have checked that $\delta\Delta_2/\langle\Delta_2\rangle$ has a weak r_s dependence for $r_s > 1$, in agreement with findings of reference [5]. This confirms that peak spacing fluctuations are dominated by capacitance fluctuations instead of single particle fluctuations.

We point out that our data are limited to spinless fermions. Interesting interaction-induced spin effects have been recently reported in experiments [27] and theoretically investigated [28–30].

5 First energy excitation

We have calculated the first N-body energy levels E_i, $(i = 0, 1, 2, ...)$ for different sizes L, with a large disorder to hopping ratio $W/t = 15$ imposed to have Anderson localization and Poissonian spectral statistics for the one particle levels at $r_s = 0$ when $L \geq 8$. We studied $N = 4, 9$, and 16 particles inside clusters of size $L = 8, 12$, and 16 respectively. This corresponds to a constant low filling factor $n_e = 1/16$. We studied an ensemble of 10^4 disorder configurations.

The first average spacing $\langle\Delta E_0\rangle$ is given in Figure 7. It exhibits a power law decay as L increases, with an exponent β given in the inset. One finds for the first spacing that β linearly decreases from $d = 2$ to 1 when r_s increases from 0 to 3. The next mean spacings $\langle\Delta E_i\rangle = \langle E_{i+1} - E_i\rangle$ depend more weakly on r_s, as shown in Figure 7.

For $r_s = 0$, the distribution of the first spacing $s = \Delta E_0/\langle\Delta E_0\rangle$ becomes closer and closer to the Poisson distribution $P_P(s)$ when L increases, as it should be for an Anderson insulator. For a larger r_s, the distribution seems to become close to the Wigner surmise $P_W(s)$ characteristic of level repulsion in Random Matrix Theory, as

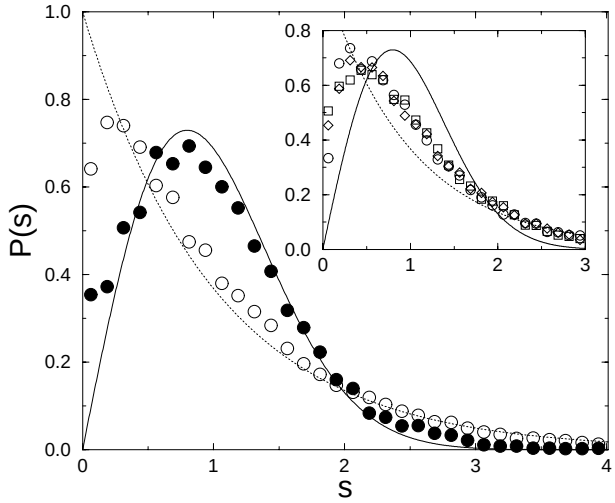

Fig. 8. Gap distribution $P(s)$ for $r_s = 0$ (empty circles) and $r_s = 2.8$ (filled circles) when $N = 16$, $L = 16$, $W = 15$, compared to $P_P(s)$ and $P_W(s)$. Inset: size invariant $P(s)$ at $r_s^C \approx 1.2$; $L = 8$ (circles), 12 (squares), and 16 (diamonds).

shown in Figure 8 for $r_s = 2.8$ and $L = 16$. To study how this $P(s)$ goes from Poisson to a Wigner-like distribution when r_s increases, we have calculated a parameter η which decreases from 1 to 0 when $P(s)$ goes from Poisson to Wigner:

$$\eta = \frac{\mathrm{var}(P(s)) - \mathrm{var}(P_W(s))}{\mathrm{var}(P_P(s)) - \mathrm{var}(P_W(s))}, \tag{11}$$

where $\mathrm{var}(P(s))$ denotes the variance of $P(s)$, $\mathrm{var}(P_P(s)) = 1$ and $\mathrm{var}(P_W(s)) = 0.273$. In Figure 9, one can see that the three curves $\eta(r_s)$ characterizing the first spacing for $L = 8, 12, 16$ intersect at a critical value

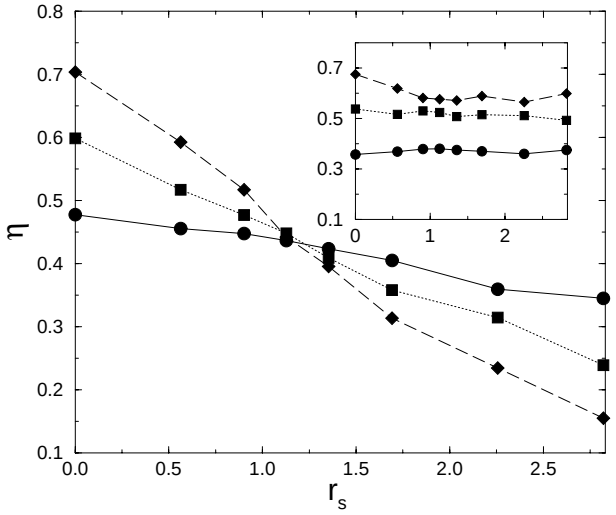

Fig. 9. Parameter $\eta(r_s)$ corresponding to the first spacing ΔE_0 at $n_e = 1/16$, $W = 15$, $L = 8$ (circles), 12 (squares), and 16 (diamonds). Inset: $\eta(r_s)$ for the second spacing ΔE_1.

$r_s^C \approx 1.2$. Our data suggest that for $r_s < r_s^C$ the distribution tends to Poisson in the thermodynamic limit, while for $r_s > r_s^C$ it tends to a Wigner-like behavior [31]. At the threshold r_s^C, there is a size-independent intermediate distribution shown in the inset of Figure 8, exhibiting level repulsion at small s followed by a $\exp(-as)$ decay at large s with $a \approx 1.52$. This Poisson-Wigner transition characterizes only the first spacing, the distributions of the next spacings being quite different. The inset of Figure 9 does not show an intersection for the parameter η calculated with the second spacing. The second excitation is less localized than the first one when $r_s = 0$, since the one particle localization length weakly increases with energy. It is only for $L = 16$ that the distribution of the second spacing becomes close to Poisson without interaction, and a weak level repulsion occurs as r_s increases.

The observed transition, and the difference between the first spacing and the following ones is mainly an effect of the HF mean field. For the first spacing, the curves η calculated with the HF data are qualitatively the same. At the mean field level the low energy excitations are particle-hole excitations starting from the ground state. The energy spacing between the first and the second excited states is given by the difference of two particle-hole excitations and a Poisson distribution follows if the low energy particle-hole excitations are uncorrelated.

Notice that the energy of an electron-hole pair is given by $\epsilon_j - \epsilon_i - U/r_{ij}$ and the classical argument for the existence of a gap in the single particle density of states does not apply [8]. For example, in the constant interaction model one pays a gap e^2/C in the single particle density of states but not in the many-body excitation spectrum ($\Delta E_0 = \Delta E_0(U = 0) \propto 1/L^2$). Therefore the observed opening of a gap for the first energy excitation is a remarkable phenomenon beyond the predictions of the classical Coulomb gap model.

6 Hopping conductivity

In disordered insulators, a crossover [8] in the temperature dependence of the resistivity $\rho(T)$ is induced by Coulomb repulsion from the Mott variable range hopping law ($\rho(T) = \rho_M \exp(T_0/T)^{1/3}$ in 2d) to the Efros-Shklovskii behavior ($\rho(T) = \rho_{ES} \exp(T_{ES}/T)^{1/2}$).

The usual argument is to consider the length $L(T)$ which maximizes the probability P_{ij} of a single particle hop from a state with energy ϵ_i to a state with energy ϵ_j:

$$P_{ij} \propto \exp\left(-\frac{2L}{\xi} - \frac{\epsilon_j - \epsilon_i}{kT}\right), \tag{12}$$

with ξ localization length.

To measure possible delocalization effects, we have calculated for $W = 15$ the number of occupied sites per particle $\xi_s = N/\sum_i \rho_i^2$, where $\rho_i = \langle\Psi_0|n_i|\Psi_0\rangle$ is the charge density of the ground state at the site i. Around $r_s \approx 1.2$ and after ensemble average, the maximum increase of ξ_s compared to $r_s = 0$ is small (2%). Therefore noticeable effects come mainly from the mean and the distribution of the single particle density of states around the Fermi level.

At low temperatures, hopping conductivity involves states near the Fermi level. If one takes for the Coulomb gap its average value $\epsilon_{N+1} - \epsilon_N \approx \Delta_2 \approx (A + Br_s)/L^{\alpha(r_s)}$ (see Fig. 4), one obtains for the hopping resistivity a smooth and continuous crossover from Mott to Efros-Shklovskii hopping, given by:

$$\rho(T) \propto \exp\left(\frac{T(r_s)}{T}\right)^{1/(\alpha+1)}, \tag{13}$$

where

$$T(r_s) \approx \frac{A + Br_s}{k\xi^\alpha}\,. \tag{14}$$

This prediction neglects the crossover from the Poisson distribution to a Gaussian distribution in the inverse compressibility (see Fig. 5), which could be included by considering for Δ_2 a more typical value than its average, for instance the value $\Delta_2(b)$ for which $\int_0^{\Delta_2(b)} P(\Delta_2')\mathrm{d}\Delta_2' = b$, with $b = 1/2$ for example. This would introduce a crossover in $T(r_s)$ around $r_s \approx 1$.

The existence of a critical r_s value for the opening of the Coulomb gap can be understood similarly to [32]. The single particle density of states around the Fermi energy E_F is given by [8] $\rho(E) \approx |E - E_F|/U^2$ and the gap size $\Delta_g = |E_g - E_F|$ can be estimated from the condition $\rho(E_g) \approx \overline{\rho}$, with $\overline{\rho} \approx 1/W$ mean density of states for $W \gg t$, obtaining $\Delta_g \approx U^2/W$. According to Fermi golden rule, the inverse lifetime of a Slater determinant built from electrons localized at given sites is $\Gamma_t \approx t^2(1/W)(N/L^2)$, with $N/(WL^2)$ density of states directly coupled by the hopping term of the Hamiltonian (1). This argument suggests that quantum fluctuations can melt the Coulomb gap for $\Gamma_t \approx \Delta_g$, giving $r_s \approx 1$. Therefore a crossover from Efros-Shklovskii to Mott hopping

conductivity is expected not only by increasing the temperature but also by increasing the carrier density, as observed in [11] at $r_s \approx 1.7$.

Notice that in the above arguments we have considered only the excitations leading to the Efros-Shklovskii behavior for the hopping conductivity, that correspond to the withdrawal of one electron or its addition to the system. However, a single electron hop may reorganize the location of the other particles, inducing complex many particle excitations (see Fig. 2, showing that simple HF is unable to reproduce the mean first many-body energy spacing when $r_s > 1$). Therefore one cannot exclude that correlated hops involving more than one particle affect the hopping conductivity [8].

7 Conclusions

In summary, we have analyzed the inverse compressibility and the first energy excitation statistics for spinless fermions in weakly and strongly disordered squared lattices when r_s increases from 0 to 3. On one hand, we have found a crossover in the electronic inverse compressibility from a $1/L^2$ towards a $1/L$ decay; at the same time its distribution evolves towards a Gaussian shape. On the contrary, our data for the first many-body energy spacing are consistent with a smooth opening of a gap and a sharp interaction-induced Poisson-Wigner-like transition in its distribution at $r_s^C \approx 1.2$, with a scale invariant distribution at the critical point showing intermediate statistics. For those small values of r_s, the ground state energy is essentially given by an effective Hartree-Fock mean field. We underline that the intermediate quantum regime discussed in reference [12] and charge crystallization occur for larger r_s factors, where the mean-field approximation breaks down and the configuration interaction method ceases to efficiently converge. This does not allow us to study the regime characterizing the experiments reported in references [3,4].

Partial support from the TMR network "Phase Coherent Dynamics of Hybrid Nanostructures" of the European Union is gratefully acknowledged.

References

1. *Disorder and Interaction in Transport Phenomena*, edited by M. Schreiber, Ann. Phys. (Leipzig) **8**, Numbers 7-9 and Special Issue (1999).
2. S.V. Kravchenko, T.M. Klapwijk, Phys. Rev. Lett. **84**, 2909 (2000), and references therein.
3. S.C. Dultz, H.W. Jiang, Phys. Rev. Lett. **84**, 4689 (2000).
4. S. Ilani, A. Yacoby, D. Mahalu, H. Shtrikman, Phys. Rev. Lett. **84**, 3133 (2000).
5. U. Sivan, R. Berkovits, Y. Aloni, O. Prus, A. Auerbach, G. Ben-Yoseph, Phys. Rev. Lett. **77**, 1123 (1996).
6. S.R. Patel, S.M. Cronenwett, D.R. Stewart, A.G. Huibers, C.M. Marcus, C.I. Duruöz, J.S. Harris Jr., K. Campman, A.C. Gossard, Phys. Rev. Lett. **80**, 4522 (1998).
7. F. Simmel, D. Abusch-Magder, D.A. Wharam, M.A. Kastner, J.P. Kotthaus, Phys. Rev. B **59**, R10441 (1999).
8. A.L. Efros, B.I. Shklovskii, J. Phys. C **8**, L49 (1975); M. Pollak, Philos. Mag. B **65**, 657 (1992); see also *Electron-Electron Interactions in Disordered Systems*, edited by A.L. Efros, M. Pollak (North-Holland, Amsterdam, 1985).
9. J.G. Massey, M. Lee, Phys. Rev. Lett. **75**, 4266 (1995).
10. H.B. Chan, P.I. Glicofridis, R.C. Ashoori, M.R. Melloch, Phys. Rev. Lett. **79**, 2867 (1997).
11. S.I. Khondaker, I.S. Shlimak, J.T. Nicholls, M. Pepper, D.A. Ritchie, Phys. Rev. B **59**, 4580 (1999).
12. G. Benenti, X. Waintal, J.-L. Pichard, Phys. Rev. Lett. **83**, 1826 (1999).
13. M. Eto, H. Kamimura, Phys. Rev. Lett. **61**, 2790 (1988).
14. T. Vojta, F. Epperlein, M. Schreiber, Phys. Rev. Lett. **81**, 4212 (1998).
15. P. Fulde, *Electron Correlations in Molecules and Solids* (Springer, Berlin, 1995).
16. B.I. Shklovskii, B. Shapiro, B.R. Sears, P. Lambrianides, H.B. Shore, Phys. Rev. B **47**, 11487 (1993).
17. H. Kato, D. Yoshioka, Phys. Rev. B **50**, 4943 (1994).
18. G. Bouzerar, D. Poilblanc, J. Phys. I France **7**, 877 (1997).
19. F. Epperlein, M. Schreiber, T. Vojta, Phys. Rev. B **56**, 5890 (1997); Phys. Status Solidi (b) **205**, 233 (1998).
20. S. Levit, D. Orgad, Phys. Rev. B **60**, 5549 (1999).
21. P.N. Walker, G. Montambaux, Y. Gefen, Phys. Rev. B **60**, 2541 (1999).
22. A. Cohen, K. Richter, R. Berkovits, Phys. Rev. B **60**, 2536 (1999).
23. Y. Alhassid, Ph. Jacquod, A. Wobst, Phys. Rev. B **61**, R13357 (2000).
24. See references [20–22] for a thorough discussion about the limits of validity of the Koopmans' theorem for disordered quantum dots.
25. R. Berkovits, B.L. Altshuler, Phys. Rev. B **55**, 5297 (1997).
26. Ya.M. Blanter, A.D. Mirlin, B.A. Muzykantskii, Phys. Rev. Lett. **78**, 2449 (1997).
27. S. Lüscher, T. Heinzel, K. Ensslin, W. Wegscheider, M. Bichler, `cond-mat/0002226`.
28. P.W. Brouwer, Y. Oreg, B.I. Halperin, Phys. Rev. B **60**, R13977 (1999).
29. H.U. Baranger, D. Ullmo, L.I. Glazman, Phys. Rev. B **61**, R2425 (2000).
30. Ph. Jacquod, A.D. Stone, Phys. Rev. Lett. **84**, 3938 (2000).
31. A similar change of gap distribution with interaction has been seen for quantum spin glasses in B. Georgeot, D.L. Shepelyansky, Phys. Rev. Lett. **81**, 5129 (1998).
32. A.A. Pastor, V. Dobrosavljević, Phys. Rev. Lett. **83**, 4642 (1999).